Temperature dependent micromechanics-based friction model for cold stamping processes

IOP Conf. Series: Journal of Physics: Conf. Series **1063** (2018) 012136 doi:10.1088/1742-6596/1063/1/012136

Temperature dependent micromechanics-based friction model for cold stamping processes

C Wang[1], J Hazrati[1], M B de Rooij[2], M Veldhuis[3], B Aha[4], E Georgiou[5], D Drees[5], A H van den Boogaard[1]

[1] Nonlinear Solid Mechanics, Faculty of Engineering Technology, University of Twente, Enschede, The Netherlands
[2] Laboratory for Surface Technology and Tribology, Faculty of Engineering Technology, University of Twente, Enschede, The Netherlands
[3] Philips, High Tech Campus 5, 5656AE Eindhoven, The Netherlands
[4] Zeller+Gmelin GmbH & Co. KG, 73054 Eislingen/Fils, Germany
[5] Falex Tribology, Rotselaar, Belgium

Corresponding author's Email: c.wang@utwente.nl

Abstract. Temperature rise in cold stamping processes due to frictional heating and plastic deformation of sheet metal alters the tool-sheet metal tribosystem. This is more prominent in forming advanced high strength steels and multi-stage forming operations where the temperature on the tool surface can rise significantly. The rise in temperature directly affects the friction due to break down of lubricant, change in physical properties of tribolayers and material behavior. This can result in formability issues such as workpiece-splitting, etc. Therefore, it is important to account for temperature effects on friction in sheet metal forming analyses. In this study, the temperature effect was included in a micromechanics-based friction model which allows calculation of local friction coefficients as a function of contact pressure, bulk strain and relative sliding velocity. The temperature influence on friction was introduced through material behavior of sheet metal, viscosity of lubricant and shear strength of boundary layer in the micromechanics-based model. The model validation has been done by comparing the calculated fractional real contact area with the experimental results. The model can be used in formability analyses and to predict optimum stamping press parameters such as the blank holder force and the press speed.

1. Introduction

Cold stamping processes, such as blanking, bending, drawing, flanging, etc., offer a variety of possibilities to form the sheet metal into a desired net shape in a cost-effective way. Nowadays, stamping processes are optimized by coupling optimization algorithms and finite element (FE) simulations to reduce material waste and improve product quality [1, 2]. The stress-strain and frictional behavior of sheet metal is key to a predictable process. Therefore, an adequate description of tribological conditions is needed to enhance the metal forming simulations [3]. Friction depends on mechanical properties of the used material, the type of lubricant, interface properties of the contacting surfaces as well as the local process parameters, such as nominal contact pressure and relative sliding velocity [4]. To enable more accurate metal forming simulations, a micromechanics-based friction model has been developed for isothermal conditions [5, 6]. The current trend in the sheet metal forming industry requires flexible production and instantaneous process stability as customization and restriction on stocks in the manufacturing industry decreases the number of products per run [7].

Defects in cold stamped products are commonly found during the start-up of the production line. This has been mainly attributed to an increase of temperature and a change of friction for an increased number of stamped parts. The temperature transient effect on friction which leads to product failures has been investigated experimentally and numerically at macroscopic level [8, 9]. However, the surface related micro-mechanisms are not considered in previous studies. In this study, the effects of temperature on frictional behavior of sheet metal-tool contact system are investigated. These effects are implemented in an existing micromechanics-based friction model. The enhanced model accounts for the temperature effects on the sheet metal material behavior, lubricant viscosity and boundary layer shear strength.

2. Model description and calibration

2.1. Micromechanics-based friction model

It has been demonstrated that the simple Coulomb friction model used in FE analyses of metal forming processes would not lead to accurate predictions [3]. Recently a numerical framework which combined several microscopic contact models has been developed to describe microscopic friction behavior on a macroscopic level, i.e. a multi-scale approach [6, 10]. The boundary lubrication model of this framework can be briefly summarized in three major steps as shown in Figure 1.

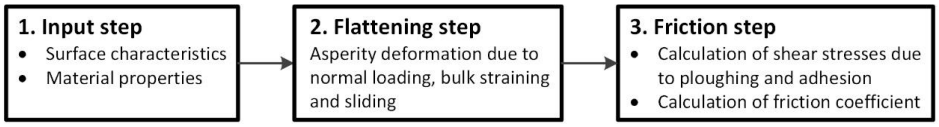

Figure 1. Solving scheme of multi-scale friction model.

2.2. Surface characteristics

The workpiece material used for this investigation, AISI 420 is a martensitic stainless steel in a stable ferritic state. The tool grade is Ceratizit CF-S18Z. Confocal microscopy measurements were performed to obtain 3D surface scans of the workpiece and the tools. The raw data of surface textures is post-processed as follows. First, a noise filter is used to remove the spikes from the measured data. Second, the noise free data are shifted and tilted to its origin. The details of these procedures can be found in [6]. The corrected surface texture of the workpiece is shown as in Figure 2. The corresponding height distribution is plotted with a B-spline fit in Figure 3. The value of arithmetic average roughness (Ra) of the workpiece and the tool surface is 0.31 µm and 0.12 µm respectively.

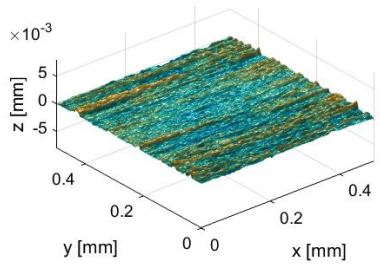

Figure 2. 3D surface impression measured by confocal microscopy.

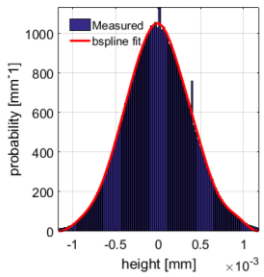

Figure 3. Measured surface height distribution and a B-spline fit.

2.3. Material property

The modified Bergström model is considered in this study as a physically-based hardening rule to describe temperature and strain rate dependence [11]. In this model the total flow stress is defined as a function of strain, strain rate and temperature:

$$\sigma_f = \sigma_0 + \Delta\sigma_m \left\{\beta(\varepsilon_0 + \varepsilon) + \left[1 - e^{-\Omega(\varepsilon_0+\varepsilon)}\right]^n\right\} + {\sigma_0}^* \left[1 + \frac{kT}{\Delta G_0}\ln\left(\frac{\dot{\varepsilon}}{\dot{\varepsilon}_0}\right)\right]^m \quad (1)$$

The nomenclature of the parameters is listed in Table 1. The hardening rule is based on the theory of multiplication of dislocations and the resistance of obstacles against movement of dislocations.

Table 1. Nomenclature of modified Bergström model.

σ_0	Static yield stress of dislocation free material	Ω	Remobilization parameter
$\Delta\sigma_m$	Stress increment parameter	${\sigma_0}^*$	Maximum dynamic stress
β	Linear hardening parameter	n	Strain hardening exponent
ε_0	Initial strain	k	Boltzmann's constant
ε	Equivalent strain	T	Temperature
$\dot{\varepsilon}_0$	Initial strain rate	ΔG_0	Activation energy
$\dot{\varepsilon}$	Equivalent strain rate	m	Dynamic stress exponent

The tensile tests of AISI420 were performed at elevated temperatures and different strain rates. The results demonstrate the temperature and strain rate sensitivity of the material. The modified Bergström hardening rule was calibrated to the experimental results. A comparison between the experimental and the fitted numerical true stress-strain curves is shown in Figure 4.

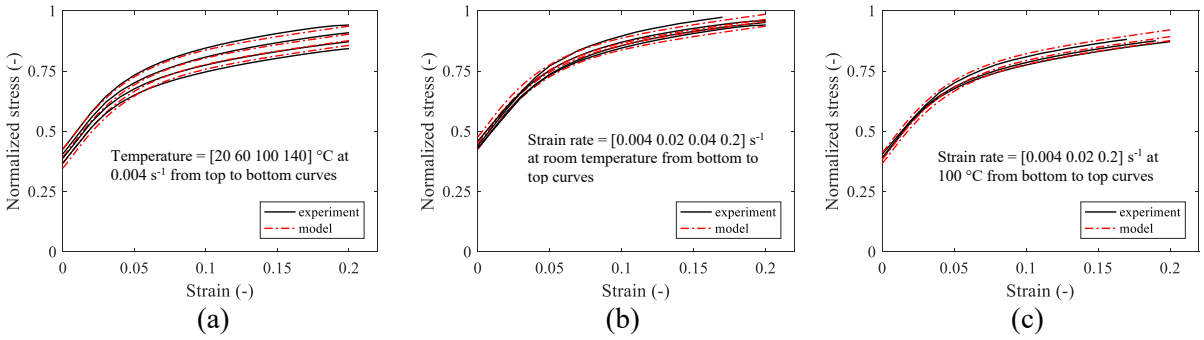

Figure 4. Calibrated numerical flow curves compared with experimental ones: (a) results on temperature dependence and (b)(c) results on strain rate dependence.

2.4. Viscosity of lubricant

It is known that lubricant viscosity tends to decrease as its temperature increases. The lubricant used for this study is Castrol Iloform FST16, which has a high amount of extreme pressure (EP) additives. EP additives in lubricants can decrease wear in the forming dies that are exposed to very high contact pressures. An exponential viscosity–temperature function is used here:

$$\eta = a \cdot \exp(-b \cdot T) \tag{2}$$

where η is the kinematic viscosity of the lubricant, T is the temperature of the lubricant, a and b are the fitting parameters for a certain type of lubricant (1.1693×10^{10} mm^2/s and 0.0578 K^{-1} here). The kinematic viscosity of lubricant was measured at different temperatures. These were used to fit the constants of the viscosity-temperature relation. The density of the lubricant was measured (9.41×10^5 g/m^3) and the dynamic viscosity is used in the friction model.

2.5. Shear strength of boundary layer

Boundary layer refers to a thin lubricant layer of molecular thickness that separates the contacting surface asperities by which the load is carried in the boundary lubrication regime [12]. The force required to shear this boundary layer is consequently defined as the so-called boundary layer shear strength (BLSS). In this study, the BLSS-temperature relation is determined by coupling the temperature dependent micromechanics-based friction model with FE simulations of the strip-drawing test.

2.5.1. Strip drawing test. Flat-die strip-drawing is a test method to measure the friction coefficients of a specific tribosystem under different process conditions, i.e., nominal contact pressure, relative sliding velocity and temperature. In this study, the friction measurements were performed with a test stand developed at FILZEK TRIBOtech and Darmstadt University of Technology [9], see Figure 5. The test conditions and the geometric parameters are summarized in Table 2.

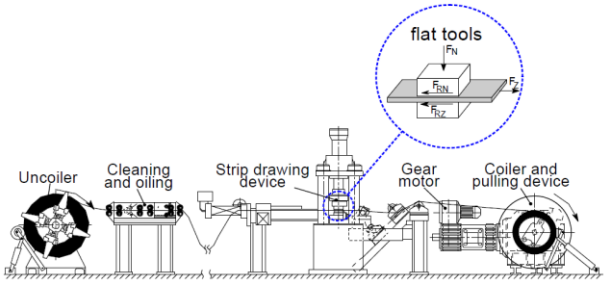

Figure 5. Schematic illustration of the strip-drawing test stand [9].

Table 2. Test conditions and geometric parameters of strip-drawing test.

Nominal pressure (MPa)	5.0, 7.5, 10.0, 12.5 15.0	Contact area (mm^2)	70×20
Temperature (ºC)	20, 40, 60 ,80	Strip width (mm)	38
Sliding velocity (mm/s)	50	Strip length(mm)	800
Lubricant amount (g/m^2)	0.6	Die radius(mm)	2

2.5.2. FE simulation and model calibration. A FE model of the strip-drawing test was built in an in-house FE software (DIEKA) during this study. The FE model accounts for hydrodynamic behaviour of lubricant during strip-drawing tests by utilizing a mixed lubrication interface element [10]. Although a small amount of lubricant (0.6 g/m^2) was applied in the experiment, simulation results showed the lubricant pressure build-up as the roughness of the AISI420 sheet surface is very low (0.3 µm, see section 2.2). This indicates the mixed lubrication regime should be considered for the model calibration of BLSS. Therefore, the FE simulations were conducted at all aforementioned experimental conditions to calibrate the temperature dependent BLSS model:

$$\tau = C \cdot {H_{eff}}^{n} \cdot \exp(\beta \cdot T) \tag{3a}$$

with

$$H_{eff} = \frac{P_{nom}}{\alpha} \tag{3b}$$

where τ is BLSS, H_{eff} is the effective hardness, P_{nom} is the nominal contact pressure, α is the fractional real contact area [6], T is the temperature and C, n and β are the calibration parameters. The power-law relation for the pressure dependence is proposed by Timsit and Pelow [13]. The exponential relation for the temperature dependence is inspired by the Arrhenius equation for the temperature dependence of reaction rates.

The calibration parameters are determined by an optimization operation. The root mean square error between the friction coefficients calculated from the FE simulations and the friction coefficients measured from experiments is considered as the objective function. This minimization problem is then solved by an optimization solver in which the temperature dependent friction model and FE model of strip-drawing test in DIEKA are coupled. At each iteration, the micromechanics-based friction model generates a friction matrix (friction coefficient as a function of pressure, strain and temperature) using the current optimal parameter set. This friction matrix is then taken as an input to run strip-drawing simulations in DIEKA and the frictional forces in the mixed lubrication regime are calculated. The friction coefficients obtained from FE analyses for all conditions are ultimately compared with the experimental results when the optimum is found for a drawing velocity of 50 mm/s and a lubricant amount of 0.6 g/m^2 (see Figure 6). Figure 7 shows the distribution of lubricant pressure between the

sheet and the flat die during the drawing process. Asperity flattening takes place in the contact area resulting in the pressure build-up in the lubricant.

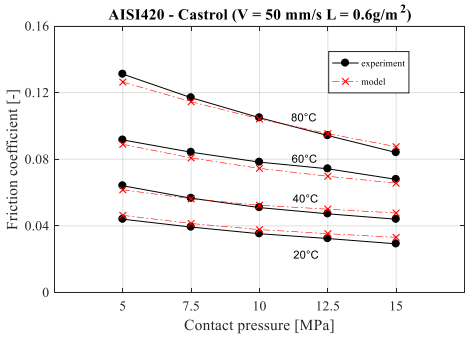

Figure 6. Friction coefficients calculated from FE model compared with experimental ones. Optimum is found at parameter set: [C n β] = [0.0104 0.0035 0.0250].

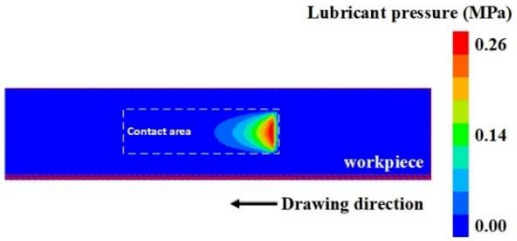

Figure 7. Lubricant pressure distribution from FE simulation at nominal pressure 5 MPa and temperature 80 ºC.

3. Results of fractional real contact area

To further check the reliability of the model, the fractional real area of contact predicted from FE analyses are compared with the real area of contact values measured in experiments. The real area of contact between sheet metal and tooling is developed due to flattening of asperities during normal loading and sliding. During strip-drawing, the real area of contact grows by increasing nominal contact pressure and by ploughing of tool asperities through contact patches on the sheet metal surface (junction growth) [14]. However, bulk strain effects on asperity flattening and real area of contact are neglected since the sheet metal strips are not deforming during the strip-drawing test. In general low pressure levels were applied during the strip-drawing test in order to ensure no adhesion between the tool and the sheet material. Therefore, the hightest pressure of 15 MPa in the experiments is taken as a feasible condition for the comparision. With the aid of confocal measurements on the virgin and deformed sheets, the height distribution can be determined as shown in Figure 8. Based on flattened asperities the fractional real contact area is obtained by calculating the fraction of cumulative probabilities in Figure 8 [5]. A comparsion between the model results and experimentally obtained ones is displayed in Figure 9. The BLSS increases with increasing temperature resulting in an increase in junction growth.

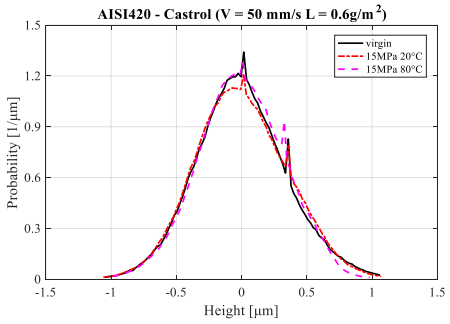

Figure 8. Surface height distribution of virgin and deformed sheet from experiment.

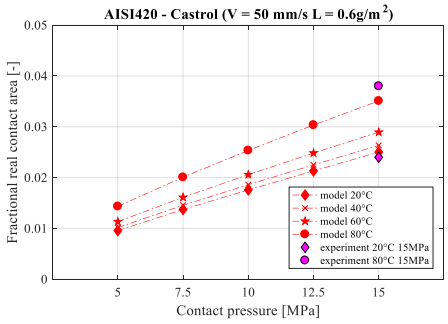

Figure 9. Comparison of fractional real contact area between model and experiment.

4. Discussion and conclusions

The temperature effect has been introduced through material behavior of sheet metal, viscosity of lubricant and shear strength of boundary layer in the micromechanics-based model. The material

model obtained is able to capture the temperature, strain rate and strain hardening effects. However, the latter is absent in strip-drawing tests and more relevant in sheet metal forming applications. The viscosity function used in this study takes temperature effects into account using an empirical relationship. More advanced viscosity models require in-depth knowledge of the chemical composition of the lubricant. As the complicated behaviors of boundary layer is still poorly understood in literature, the shear strength of the boundary layer as a function of pressure and temperature has been fitted to the strip-drawing friction tests adopting a reverse engineering approach. Simulation results show that despite a small amount of lubricant at the contact, part of the load is carried by lubricant due to the rather smooth surface of AISI420 sheet. This means the FE simulations of strip-drawing test in the mixed lubrication friction regime are needed to properly calibrate the boundary layer shear strength model. In addition, the lubricant pressure can also be predicted by the numerical model. From the calculated lubricant pressure distribution, the wedge effect introduced by the die radius can be clearly observed. In summary, the combination of the micromechanics-based friction model and the FE model is able to reproduce the temperature effect on the friction evolution. The reliability of the model is checked by comparing real contact area predictions with the measured values from experiments. However, in the future work the model will be validated using sheet metal forming applications.

Acknowledgments
This research was carried out within the project “ASPECT – Advanced Simulation and control of tribology in metal forming Processes for the North West European Consumer goods and Transport sectors”, cofounded by the INTERREG North West Europe program (www.nweurope.eu/aspect).

References
[1] Meinders VT, Burchitz IA, Bonte MHA and Lingbeek RA 2008 Numerical product design: springback prediction, compensation and optimization *Int. J. Mach. Tool Manufact.* **48** 5 p 499-514
[2] Havinga GT, Boogaard AH van den and Klaseboer G 2017 Sequential improvement for robust optimization using an uncertainty measure for radial basis functions *Struct. Multidiscipl. Optim.* **55** 4 p 1345-1363
[3] Roll K 2008 *Proc. the 7th Int. Conf. on Numerical Simulation of 3D Sheet Metal Forming Processes (Sept. 1-5 Interlaken)* p 3
[4] Altan T and Takkaya E editors 2012 *Sheet Metal Forming Fundamentals* (ASM International)
[5] Karupannasamy DK, Hol J, Rooij MB de, Meinders VT and Schipper DJ 2012 Modelling mixed lubrication for deep drawing processes *Wear* **294-295** p 296-304
[6] Hol J, Meinders VT, Rooij MB de and Boogaard AH van den 2015 Multi-scale friction modelling for sheet metal forming: the boundary lubrication regime *Tribol. Int.* **81** p 112-128
[7] Meinhardt J 2012 *Forming in Car Body Engr. Conf. (Sept. 26-27 Bad Nauheim)*
[8] Grüebler R and Hora P 2009 Temperature dependent friction modelling for sheet metal forming *Int. J. Mater. Form.* **2** p 251-254
[9] Filzek F, Ludweg M and Groche P 2011 *Proc. the 15th Int. Deep Drawing Research Group Conf. (Jun. 5-8 Bilbao)*
[10] Hol J, Meinders VT, Geijselaers HJM and Boogaard AH van den 2015 Multi-scale friction modelling for sheet metal forming: the mixed lubrication regime *Tribol. Int.* **85** p 10-25
[11] Liempt P van 1994 Workhardening and Substructural Geometry of Metals *J. Mater. Process. Tech.* **45** p 459-464
[12] Sethuramiah A 2003 Boundary lubrication mechanisms metallic materials *Tribol. Series* **42** p 99-131
[13] Timsit RS and Pelow CV 1992 Shear strength and tribological properties of stearic acid films (part 1) on glass and aluminium-coated glass *J. Tribol.*, **114** p 150-158
[14] Tabor D 1959 Junction growth in metallic friction: The role of combined stresses and surface contamination *Proc. Royal Soc. Lond.* **251** p 378-393